4

Application of Airborne Sound Waves for Mass Transfer Enhancement

Sergey V. Komarov
Nippon Light Metal Company, Ltd.
Japan

1. Introduction

Efforts to reduce energy use and greenhouse gas emissions continue to place increasingly stringent requirements on the industrial sector of the economy. This tendency is especially pronounced in energy-intensive industries which use high temperature processing. Examples are chemical and metallurgical processes, power generation and waste treatment. In these areas, many chemical reactions involved in the material fabrication or treatment proceed under mass transfer control, meaning that rate-controlling step of the reactions is not a chemical reaction itself (termed kinetic control), but transport of the chemical reagents to or from the reaction zone. This is associated with the well-known fact that the rates of chemical reactions increase with temperature to a greater extent than those of mass transfer. In the mass transfer controlling regime, any enhancement of the mass transfer rate should raise productivity of the above-mentioned processes, that in turn provides an option to reduce the energy consumption and production cost. Another important point to note is that inadequate control of mass transfer between different regions of the reactors or furnaces often results in a local under- or overheating of the materials being processed. Both these phenomena are considered to be a major source of atmospheric pollutant emissions. Typical examples of such processes are solid waste incineration and fuel combustion.

In most of the above-mentioned processes gaseous, liquid and solid phases coexist in one process. Nevertheless, in this chapter, we shall restrict our consideration to the gas-phase mass transfer. In gas, mass transfer can occur through the following two mechanisms: (1) convection which typically occurs in the gas bulk and (2) molecular diffusion which is the dominant near interfaces. In many cases, the rate of convective mass transfer can be relatively easily enhanced by blowing a gas into the media bulk or by applying some other method of increasing the forced convection. Therefore, the main resistance to the mass transfer is located usually in the boundary layers adjacent to the interfaces between different phases. Under these conditions, there is a very limited choice of techniques available for controlling the mass transfer at the interfaces. This is especially true in regard to those processes which involve high temperatures.

In these circumstances, sound or ultrasound waves provide a unique tool making it possible to supply energy directly to the interfaces and, thus, to influence the interfacial mass transfer rates. Attractiveness of ultrasonics is associated with the following features of sound. First, sound waves have the ability to propagate through homogeneous elastic mediums including gas without significant losses, and thus to effectively transfer the

acoustic energy from a sonic generator to the materials being processed. Second, when the waves are incident upon an interface, the scattering or reflecting of the waves from the interface is responsible for a number of phenomena that occur at the interfaces. Examples of these phenomena include acoustic streaming, radiation pressure, forced turbulence and capillary waves. Most of them have a direct influence on the interfacial mass transfer process. Such effects are unachievable by any other methods. Third, along with the technical efficiency, sonic/ultrasonic treatment should be competitive as regards cost, because it provides an effective transmission of acoustic energy at a relatively low cost for ultrasonic equipment.

The idea of using ultrasonics for improving process performance or for changing material structure is rather old. As early as the 1920s, Wood and Loomis (Wood & Loomis, 1927) had studied the effects of ultrasonics on the atomization of liquids, the emulsification of immiscible liquids, and the changes in the structure of crystallized organic substances. During the years which followed, ultrasonic effects have become the subject of numerous extensive studies. The studies have proved the benefits of using ultrasonics in a variety of technological processes. In the majority of them, sound waves of ultrasonic range are radiated into liquids through a submersible sonotrode under conditions in which acoustic cavitation occurs in the liquid. Ultrasonic sonochemistry, a relatively new field of chemistry, exploits the acoustic cavitation to influence chemical reactions. Acoustic cavitation is a phenomenon of nucleation, oscillation and implosion of countless bubbles in liquids. The last phenomenon, namely bubble implosion, is of great importance in many ultrasonic applications. Cumulative microjets and shock waves, which are generated at the last moment of bubble implosion are thought to be one of the main contributor to the effects observed during ultrasonic treatment. Also, the ultrasonic cavitation is a very efficient route to enhance mass transfer rates both in the bulk and at the interfaces in liquids (e.g. Margulis, 1995).

However, the liquid-phase sonoprocessing has a number of serious limitations. As ultrasound waves are scattered on gas-liquid interfaces, the surface of cavitation bubbles has a screening effect on propagating acoustic energy. This leads to a significant decrease in the size of the zone that can be effectively treated by ultrasonic. This limits the ultrasonic applications for many processes proceeding in large-size reactors. Moreover, at higher temperatures, sonoprocessing through liquid phases requires designing a cooling system, choosing special materials for the waveguide components, and optimizing them under conditions of sharp temperature drops. Unfortunately, this is not always possible

On the other hand, the gas-phase sonoprocessing possesses some advantages as compared to the treatment of liquid phases that make it very useful for applying to high-temperature processes. First, the sound generator can be positioned a safe distance away from the high temperature zone. Second, in gas, sound waves can propagate over a longer distance than that in liquids because the sound propagation in gas is not restricted by cavitation. The gas-phase sonoprocessing is especially appealing for the processes that use gas blowing or injection. Typical examples are burners, solid waste incinerators, converters for making steel and cooper. In these processes, a sound wave can be relatively easily produced by passing a part of blown gas through a pneumatic-type sound generator that does not require any additional consumption of energy. In addition, the gas can serve as a coolant of the sound generator parts.

The goal of this chapter is to give a deeper insight into the possibilities and limitations of airborne sound waves as a tool to enhance the rates of gas-phase mass transfer and its related phenomena. Following the introduction, the second section gives a brief theoretical

consideration on the sound related fundamental phenomena that is necessary for a better understanding of the following sections. The next, third section presents a short review of some recent studies that examined sound or ultrasound effects on the gas-phase mass transfer around spherical drops and particles, followed by a brief survey of recent efforts in applying acoustic oscillations to in a number of technological processes. The forth section provides a discussion of our results and some considerations for the enhancement of mass treansfer rates in pyrometallurgical processes. Finally, the last section concludes the chapter with some general remarks.

2. Brief theoretical consideration

Sound is a wave that is created by oscillating objects and that travels through an elastic medium from one location to another. The simplest type of sound wave is a plane travelling wave. The wavefront in such a wave is a plane surface meaning that the oscillating energy is transmitted in the form of parallel beam. When the oscillation amplitude is small enough (linear regime), one can neglect any interaction between the medium and wave, and consider that the wave propagates adiabatically.

In actual practice this situation is very seldom realized. In the material sonoprocessing, sound waves of high intensity propagate inside reactor vessels filled with solid and/or liquid materials, and bounded by side walls and bottom. This suggests that the wave can be reflected or absorbed by surfaces belonging to the materials or vessels. In addition, processes often generate small particulates like solid particles, dust or liquid droplets. When the travelling wave impinge on their surfaces, a part of the wave energy can be scattered and lost. Moreover, propagation of high intense sound wave is non-adiabatic because a part of its energy is lost during the compression half cycle. This phenomenon is know as disspation. The dissipation and scattering are thought to be the main cause of the wave attenuation. Besides, scattering and dissipation of waves are responsible for so-called non-linear acoustic effects which have a direct bearing on the transfer of mass. The following sections introduce most important characteristics of sound waves and, then, briefly explain the non-linear effects to that extent which is necessary for understanding the matter of the present chapter.

2.1 General characteristics of sound waves

In the case of a harmonic travelling wave, the oscillatory motion can be expressed in terms of displacement of the particle,ξ relative to their equilibrium position as follows

$$\xi = \xi_0 \sin(\omega t - kx) \tag{1}$$

This equation is the basis for derivation of other equations which describe the wave propagation. Thus, the velocity of oscillations, V, and pressure, P can be given as

$$V = V_0 \cos(\omega t - kx) \tag{2}$$

$$P = P_0 \sin(\omega t - kx) \tag{3}$$

where x is the direction of wave propagation, angular frequency $\omega = 2\pi f$ and amplitudes ξ_0, V_o, P_o are related to each other as $V_0 = \xi_0\omega$ and $P_0 = \xi_0\omega\rho c$. The wave number k can be simply defined as $k = \omega/c$ or as $k = 2\pi/\lambda$, where c and λ are the sonic velocity and wave length, respectively. Frequency, f is commonly subdivided into audible sonic and inaudible

ultrasonic ranges although physically there is no difference between sound and ultrasound waves. The boundary between these ranges lies at about 16 kHz. Note that if the travelling wave is plane and propagates without attenuation, all the amplitudes ξ_0, V_o, P_o are constant. Based on the above relationships, one can derive an expression of sound intensity, *J*, which is defined as the average rate of sound energy transmitted by a travelling wave through a unit area normal to the direction of sound propagation

$$J = \frac{1}{2}\rho c V_0^2 \tag{4}$$

In practice, since the sound intensity varies by several orders of magnitude, it is often expressed in logarithmic form known as sound intensity level,*SIL*

$$SIL = 10\log\frac{J}{J_{ref}} \tag{5}$$

where the reference intensity, J_{ref} is equal to 10^{-12} W/m^2. The unit of SIL is decibel, *dB*.
There is no universally accepted criterion for distinguishing between low and a high-intense sound waves. However, many experimental results suggest that the sonic/ultrasonic effects can be obtained only if wave amplitude exceeds some threshold value. For gases, the threshold value of V_0 can be estimated from the experimentally determined value of SIL at which ultrasonic effects become significant. This value is equal to 130 dB (Mednikov, 1965; Blinov, 1991). Thus, using Eqs.(4) and (5), one can estimate the threshold V_0 for air (c=340 m/s, ρ=1.2 kg/m^3) to be approximately 0.2 m/s.

2.2 Sound wave reflection. Standing wave.

As mentioned above, in many applications, sound waves propagate inside vessels like combustion chambers, furnaces, etc. This results in an impingement of the waves upon the vessel walls and in a reflection from the wall surfaces. Moreover, the principle of sonoprocessing itself involves exposing the surfaces of treated materials to a sound wave which, in general, can reflect from the surfaces or pass through it. In this connection, it is important to know conditions of wave reflection. When a sound wave is incident from a medium 1 on a plate made of medium 2 at right angle, the reflection coefficient, R can be expressed by the following equation (Heuter & Bolt, 1966)

$$R = \frac{\frac{1}{4}\left(m - \frac{1}{m}\right)^2 \sin^2\frac{2\pi d}{\lambda_2}}{1 + \frac{1}{4}\left(m - \frac{1}{m}\right)^2 \sin^2\frac{2\pi d}{\lambda_2}} \tag{6}.$$

Here, d is the plate thickness, λ_2 is the length of sound wave in medium 2, m is the ratio of acoustic impedances of the media 1 and 2. The acoustic impedance is a key parameter in understanding the behaviour of sound wave when incident on a surface. Generally, acoustic impedance implies resistance to the propagation of sound wave. Quantitatively, it can be expressed as the ratio of sound pressure generated in a point of medium to velocity of oscillations of the medium particles during sound propagation. Expressing the ratio in terms

of the appropriate amplitudes, one obtains the following relationship for acoustic impedance, Z

$$Z = \frac{P_0}{V_0} = \frac{\rho c V_0}{V_0} = \rho c \tag{7}$$

where ρ and c have the same notations as above. A special feature of gas phases that their acoustic impedances are several orders of magnitudes smaller than those of liquid and solid phases. For example, values of Z for air, water and steel at 20°C are 406, 1.47×10^6 and 4.56×10^7 kg/m²·c, respectively.

Insertion of these values into equations (6) and (7) gives the results illustrated in Figure 1. This figure shows the reflection coefficients as a function of d/λ_2 for two cases. In both the cases a sound wave propagates in air. However, in the first case the medium 2 is water while in the second one it is steel. As can be seen, decrease and following increase in R near $d/\lambda_2 = 0.5$ and 1.0 occurs so sharply that the corresponding descending and ascending lines are indistinguishable in the figure. The inset (b) shows an enlarged view of variation of R in the vicinity of $d/\lambda_2 = 0.5$. The data reveal that the sharp variation of R takes place within a very narrow range of d/λ_2. Besides, it is clearly seen that this variation is steeper for steel plate than for water layer. Another region of sharp change in R appears at very small d/λ_2 close to zero. Here, it can be seen again that R for steel plate increases with d/λ_2 significantly faster compared to that for water layer.

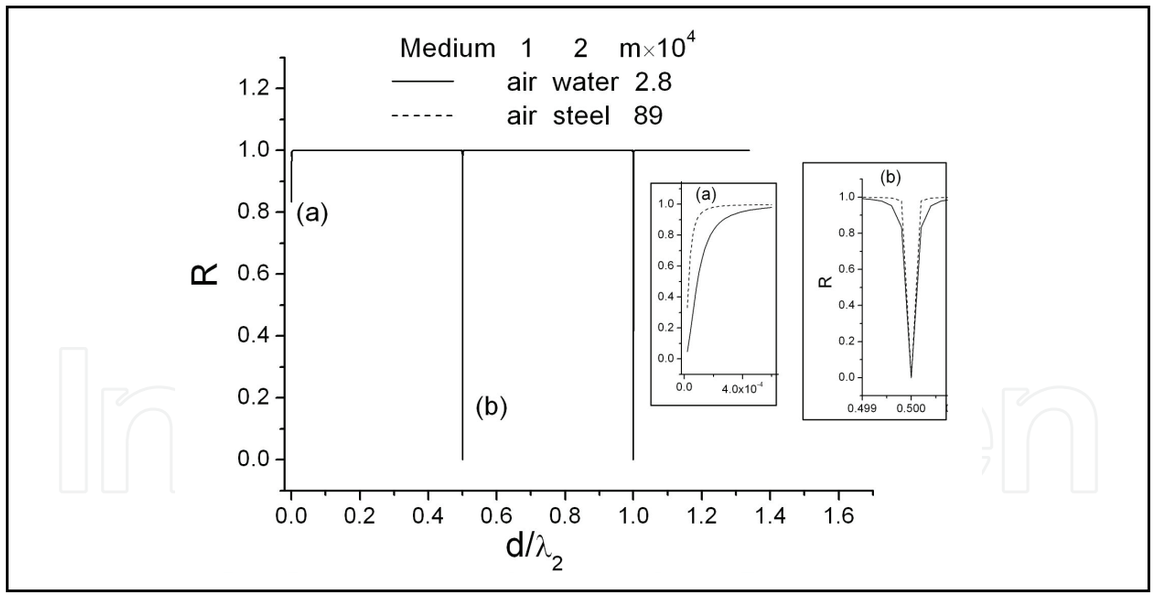

Fig. 1. Dependence of reflection coefficient on d/λ_2 for sound waves propagating in air and falling onto a water film (solid line) and a steel plate (dashed line).

Thus, one can conclude that, except for very thin films ($d/\lambda_2 \approx 0$) , sound can pass through a bulk layer of liquid or solid only when the layer thickness is varied within a very narrow range around strictly fixed values. In practice, such cases, however, are few and far between. Therefore, it can be said that when a sound wave is introduced into a vessel filled with materials to be processed, the wave is completely reflected from all surfaces on which it is

incident. The interference between incident and reflected waves may result in formation of so-called standing wave. Since the standing waves play an important role in the airborne sonoprocessing, it is necessary to consider this problem in some detail.

The simplest case of standing wave is one that forms when a travelling wave is incident upon a plane surface at right angle and completely reflected from the surface. In this standing wave, the oscillatory motion of fluid particles is expressed similarly to travelling waves in terms of displacement, oscillation velocity and sound pressure as given by Eqs.(8)~(10).

$$\xi = 2\xi_0 \cos(kx)\sin(\omega t) \tag{8}$$

$$V = 2V_0 \cos(kx)\cos(\omega t) \tag{9}$$

$$P = 2P_0 \sin(kx)\sin(\omega t) \tag{10}$$

where notations follow those of Eqs.(1)~(3).

It is remarkable that the values of amplitudes in the standing wave are double those in the travelling one. The solution of the above equations, although not shown here, reveals that, in the standing wave, there are points at which no oscillations occur. These points are referred to as node. The nodes are evenly spaced at intervals of one-half wave length. The points where the amplitude of the standing wave is a minimum are called antinodes. The antinodes occur midway between the nodes.

In standing wave, contrary to travelling one, there is no energy transfer. Instead, the energy is alternately transferred from kinetic to potential energy. By analogy with sound intensity level, *SIL*, the energy inside a standing wave can be evaluated by the sound pressure level, *SPL* in dB units as follows

$$SPL = 20\log\frac{P_0}{P_{ref}} \tag{11}$$

here the reference pressure, P_{ref} is equal to 2×10^{-5} Pa.

A special type of the standing wave occurs when it is formed between parallel surfaces, one of which is a sound-radiating surface while the other one is a reflecting surface. The longitudinal distribution of sound pressure, P in such a wave obeys the following equation (e.g. Rayleigh, 1945)

$$P = \xi_0 \omega c \rho_0 \frac{\cos k(L-x)}{\sin kL}\sin\omega t \tag{12}$$

where L is the distance between surfaces while the other notations are the same as above. Of most practical interest is the case when the distance L is an integer multiple of one-half wavelength according to Eq.(13)

$$L = \frac{n\lambda}{2},\ n = 1,2,3,... \tag{13}$$

Insertion of Eq.(13) into Eq.(12) gives $\sin kL=0$ meaning that the sound pressure P should increase to infinity. Of course it is physically impossible because of dissipative effects, the

role of which increases with the oscillation amplitude. This kind of wave, called forced resonance standing wave, is very important for practical application because it allows to achieve very high levels of sound pressure with relatively small inputs of energy. In practice, the above resonance conditions can be realized either by fixing the sound radiator at a distance of L from the reflecting surface, or by adjusting the sound frequency in such a way to satisfy the relation (13).

It is to be noted that, in practice, geometry of vessels can be more complicated than the above case of parallel surfaces. Therefore, the resonance conditions are often determined experimentally by measuring the sound pressure inside the vessel as a function of the sound frequency and vessel geometric parameters.

2.3 Attenuation of sound waves.

As has been mentioned, all the above phenomena are well described in the framework of linear acoustics without considering any influence of the surrounding medium on wave propagation. Actually, as a sound wave is propagated through a medium, its intensity is attenuated through a number of mechanisms. As a matter of fact, the wave attenuation is the main reason of non-zero net mass flux that is, in turn, a cause of the mass transfer in high-intense sound wave.

The attenuation mechanisms include scattering and dissipation. Scattering refers to the reflection or refraction of sound waves when they impinge on an obstacle with dimension close to or less than the sound wavelength. Here, by an obstacle is meant any foreign substance on the second phase, for instance particulate, acoustic impedance of which differs greatly from that of the surrounding medium. Despite the fact that mechanism of scattering is very complicated, different theoretical considerations and experimental observations suggest similar relationships between the intensity of scattering and three key parameters: sound frequency, f, obstacle dimension, d and its mass fraction, C_o. Thus, Landau and Lifshits (Landau & Lifshits,1986) derived a formula which suggests that the intensity of scattering,I_s is proportional to the sixth power of d and fourth power of f for the case of rigid particles suspended in a gas. The reported dependences of I_s on C_o are linear for both the gaseous (Temkin, 1998) and liquid mediums (Carlson & Martinsson, 2002). Therefore, the intensity of scattering becomes significant only at higher frequencies, generally in the MHz range and/or at larger volume fractions of particulates. Since the commonly used frequency ranges in the airborne sonoprocessing do not exceed several tens kHz and because the fraction of particles, which can present in gas phases, is rather small, influence of scattering on the wave propagation will be neglected in the present discussion. However, it is to be noted that the scattering is of fundamental importance in considering the behavior of the particles themselves.

Sound energy dissipation, or absorption, is assumed to be the main cause of sound intensity attenuation in most of the applications considered in the present chapter. Generally, there are two main mechanisms of sound energy absorption in fluids. These are viscous dissipation, that occurs due to the normal and shear stresses induced in fluids on sound wave propagation, and heat conduction, that results from non-adiabatic nature of heat transfer during compression and rarefaction cycles in sound wave. Both these mechanism contribute the sound energy dissipation that can be expressed quantitatively in terms of the absorption coefficient, α, that is the sum of the viscosity-related term, α_V, and heat conduction-related term, α_T. For low-amplitude oscillations, α is expressed by Eq.(14)

$$\alpha = \alpha_V + \alpha_T = \frac{\omega^2}{2\rho c^3}\left(\frac{4}{3}\eta + \eta'\right) + \frac{\omega^2}{2\rho c^3}\kappa\left(\frac{1}{C_V} - \frac{1}{C_P}\right) \tag{14}$$

where $\omega = 2\pi f$, η is the shear viscosity, η′ is the bulk viscosity, κ is the thermal conductivity, C_V and C_P are the specific heats at constant volume and pressure. In this case, attenuation of sound intensity due to absorption follows the exponential law according to Eq.(15).

$$J_x = J_o e^{-2\alpha x} \tag{15}$$

where J_0 and J_x are the intensities of sound waves at two points spaced each other by a distance of x in the direction of wave propagation. As readily seen from Eq.(14), energy absorption varies in proportion to the square of the frequency, f.

Attenuation of high-amplitude sound oscillations occurs more vigorously than that of low-amplitude oscillations. The stronger attenuation is associated with the conversion of a part of initial sinusoidal wave into the energy of arising high-frequency harmonics, rather than with absorption energy. Therefore, the attenuation coefficient of high-amplitude sound wave can exceed the absorption coefficient of low-amplitude sound wave by two orders of magnitude. There are also the other reasons but their detailed consideration is beyond the scope of this chapter. The relevant information on this topic can be found in books (Abramov, 1998; Hamilton & Blackstock, 1998).

2.4 Acoustic streaming.

The sound energy attenuation is responsible for a number of non-linear effects which serve as the basis for many ultrasonically based technologies. The main acoustic nonlinear effects arising in gas-phase systems are acoustic streaming, forced vorticity, and radiation pressure.

There is a great body of literature devoded to investigations of the above effects. Detailed discussion on the results of these investigations can be found in a variety of books,e.g.(Rayleigh, 1945; Mason & Thurston, 1965; Hamilton & Blackstock, 1998; Lighthill, 2001) and reviews,e.g (Makarov & Ochmann, 1996,1997; Leighton, 2004). This section briefly outlines the acoustic streaming which is of primary importance in understanding the matter presented in the following sections.

Acoustic streaming is the steady flow that is generated in a fluid medium due to momentum transfer associated with the attenuation of a sound wave. The physical origin of acoustic streaming was best explained by Lighthill (Lighthill, 1978). Briefly, the explanation is as follows. Propagation of a sound wave causes fluctuations of the medium fluid particles at certain time scale and amplitude which are governed by the wave frequency and intensity. By applying the Reynolds stress approach to express the mean momentum flux due to the wave in the same manner as it does for turbuent pulsations, one can derive Reynolds stress, τ, in a sound wave as

$$\tau = \overline{\rho u_i u_j} \tag{16}$$

where $\boldsymbol{u}_{i,j}$ are the fluctiating velocity in the sound wave. The bar signifies a mean value. The wave attenuation results in a spatial variaton of the Reynolds stress that can cause a non-zero net force exerted on the fluid. This force is capable of generating a steady flow termed acoustic streaming.

It is generally recognized that there three types of acoustic streamings. They differ each other by the spatial scale on which they can spread. The acoustic streaming of the first type is generated in an unbounded body of fluid. In this case, the streaming is a steady flow directed away from the sonic generator in the direction of wave oscillations. As its scale can be larger compared to the sound wavelength, it is called large-scale streaming. It is generally agreed that the large-scale streaming originates from the sound energy absorption briefly considered above. Under some conditions, the velocity of this type of streaming can be as high as several m/s (Lighthill, 1978).
The acoustic streamings of the second and third types are generated in the presence of solid obstacles (walls, particulates, etc.) placed in an acoustic field. In this case, the attenuation occurs because of frictional dissipation between an oscillating gas volumes and solid surface within the resulting boundary layer. The acoustic streaming of the second type is generated outside the boundaly layer. The scale of such an outer streaming is much smaller than that of the first type, and is equal approximately to the wavelength. The acoustic streaming of the third type is called inner small-scale streaming because it is induced within the bounday layer, the dimension of which is much smaller than wavelength. The effective thickness of the boundaly layer is about 5 times larger than that of acoustic boundaly layer which is given by the following expression

$$\delta = (\nu/\omega)^{0.5} \tag{17}$$

where ν is the kinematic viscosity of fluid, ω is the angular frequency of sound, $\omega=2\pi f$ (Zarembo, 1971).

3. Combustion and environmental control applications.

3.1 Mechanisms of mass transfer enhancements

As pointed in the above section, application of acoustic oscillations can lead to the occurrence of several phenomena responsible for improvements in the gas-phase mass transfer characteristics. The persistence of the acoustic effects and their magnitude should vary from process to process depending on the gas flow pattern inside the vessel, the presence of solid or liquid particulates as well as their size, temperature and so on. Numerous studies have shown that when acoustic oscillations are imposed on homogeneous flames or gas jets, the mass transfer enhancement is achieved through an intensification of turbulent mixing and improvement in entrainment characteristics of gas flames and jets. When a process involves chemical reactions proceeding at the surfaces of particulate or bulk materials of another phase, both the turbulent mixing in the gas bulk and flow at the surfaces have been found to be important in enhancing the mass transfer.
Experimental difficulties, encountered in high-temperature measurements, have motivated researchers to conduct cold model and numerical investigations. Other studies, although not focusing specifically on high temperature processes, have attempted to clarify the effects of acoustic oscillations on mass and heat transfer at room temperatures. The results of both groups of studies are of great importance for elucidating the mechanisms of mass transfer enhancement. Of special interest are studies that examine the mass transfer at curved surfaces like spheres and cylinders.

In one of the earlier study (Larsen & Jensen, 1977), evaporation rate for single drops of distilled water was measured under sound pressure of 132~152 dB and frequency of 82~734 Hz. The drops were suspended in dry air in upward motion and subjected to a horizontal standing wave sound field. The range of drop diameter was 0.8~2 mm. The authors used two dimensionless numbers, the drop diameter based Reynolds number, Re and the Strouhal number, S to correlate them with the experimentally determined Sherwood numbers, Sh defined on the basis of drop diameter, d. The expressions for the dimensionless numbers are given below.

$$\mathrm{Re} = \frac{V_0 d}{\nu} \tag{18}$$

$$S = \frac{d}{\xi_0} \tag{19}$$

$$Sh = \frac{k_M d}{D} \tag{20}$$

Here, k_M is mass transfer coefficient, D is the diffusion coefficient. The other notations are the same as above. The Strouhal number is a dimensionless number describing the oscillation flow around the sphere. At S < 1, Sherwood number was found to be increased proportionally to the 0.75 power of Re/S. Since, if V_0 is kept constant, the displacement ξ should increase with a decrease in frequency ω, these data suggest that lower frequencies are preferable for the mass transfer enhancement at S < 1. However, as S > 1, Sherwood number increased only with the 0.2 power of ReS^2. This suggests that higher frequencies are more desirable to enhance mass transfer rate at S > 1. The perhaps most interesting finding of this work was that flow around the drops at S < 1 and S > 1 is different. In the first case, gas flows completely around the sphere during a half-cycle of acoustic oscillation. If Re is high enough, the gas oscillations result in separation of boundary layer followed by buildup and shedding of eddy structures downstream of the separation points. It is assumed that these phenomena are the main cause of the mass and transfer enhancement at S < 1. On the other hand, when S > 1, the gas particles perform relatively small oscillations around drop causing an acoustic streaming to occur at its surface.

In one of the recent investigations (Kawahara et al.,2000), a small glass sphere (diam.1.6mm), covered by 0.4 to 0.6 mm thick layers of camphor or naphthalene, was positioned at a pressure node of a ultrasonic standing wave field to determine a distribution of the mass transfer rate over the sphere surface. Since the experiments were performed under a very high frequency of 58 kHz, a strong acoustic streaming was generated around the sphere that was found to be the main reason of the mass transfer enhancement. It was shown that the mass transfer due to the acoustic streaming is a strong function of the location on the surface being a maximum at the equator and a minimum at the poles. The authors derived the following expression to calculate the averaged Sherwood number, Sh as a function of the r.m.s. amplitude of gas particle velocity, B_{rms}, ω and D.

$$Sh = 1.336\,\mathrm{Re}; \quad \mathrm{Re} = \frac{B_{rms}}{\sqrt{\omega D}} \tag{21}$$

The other notations are the same as above. Notice that in their study the Reynolds number, Re is based on the acoustic streaming velocity. Here the Strouhal number, when defined by Eq.(19) , can be estimated to be much more than 1.

In another experimental study (Sung et al., 1994), the authors investigated mass transfer from a circular cylinder of 25 mm in diameter positioned in a steady flow on which acoustic pulsations were superimposed. The cylinder surface was precoated by a thin layer of naphthalene. Contrary to the above mentioned paper (Larsen & Jensen, 1977), in this study the directions of the steady and oscillatory flows were parallel to each other. The pulsation frequency was ranged from 10 to 40 Hz. The main conclusion from their results is that the enhancement of mass transfer rate is more effective at larger pulsation amplitudes and higher frequencies due the vortex shedding. Estimates show that the Strouhal number in these experiments is more then 1.

A detailed analysis, both experimental and theoretical, of evaporation from acoustically levitated droplets of various liquids was provided by Yarin et al. (Yarin et al., 1999). In their investigation, the frequency was 56 kHz. Therefore, the Strouhal number was assumed to be much more than unit. By plotting the Sherwood numbers against the Reynolds numbers, the authors showed that all data fall well on a straight line that is in agreement with their theoretical predictions. Both the Sherwood and Reynolds numbers were defined according to Eqs.(21). It was concluded that the effect of the acoustic field on droplet evaporation appears to be related to the acoustic streaming and squeezing of the drop by the acoustic radiation pressure.

A great body of experimental studies has been performed regarding the effects of acoustic oscillations on heat transfer from various geometries and surfaces. Taking into consideration the analogy between heat and mass transfers, a brief mention of some results of these studies will be made here. As before, our main interest is to clarify the effects of sound intensity and frequency on the heat/mass transfer characteristics.

One of the earlier study (Fand & Cheng, 1962) examined the influence of sound on heat transfer from a circular cylinder in the presence of a mean crossflow. In the experiments, air was blown onto the surface of the cylinder having a diameter of 3/4 inch. Simultaneously, the cylinder surface was exposed to high-intense acoustic oscillations at two frequencies, 1100 and 1500 Hz. The experimental data were presented as plots of $\alpha=Nu_v/Nu_0$ against the crossflow Reynolds number, Re_{cf} based on the cylinder diameter and crossflow velocity. Here, Nu_v and Nu_0 are the Nusselt numbers measured in the absence and presence of acoustic oscillations, respectively. They are given as follows

$$Nu_v = \frac{h_v d}{\lambda} \qquad Nu_0 = \frac{h_0 d}{\lambda} \tag{22}$$

where h_v and h_0 are the heat transfer coefficients from the cylinder in the absence and presence of acoustic oscillations, respectively, d is the cylinder diameter and λ is the thermal conductivity. Although the authors did not mention the Strouhal number, S in their paper, using the equations of the above sections, one can estimate S to be much more than 1.

The results of this study showed the following. At Re_{cf} about 1000, which was the lowest Re_{cf} examined, a 20 per cent augmentation of α was obtained at a SPL of 146 dB regardless of frequency. The augmentation mechanism was assumed to be an interaction similar to thermoacoustic streaming. As Re_{cf} increased to about 5000, α was reduced to 1. Then, α increased again with Re_{cf} reaching a maximum value at Re_{cf} = 8000~9500 on frequency of

1100 Hz and at Re_{cf} = 9000~11000 on frequency of 1500 Hz. In these ranges of Re_{cf}, the increase in heat transfer appears to be the result of two different interactions: (1) a resonance interaction between the acoustic oscillations and the vortices shed from the cylinder; (2) a modification of the flow in the laminar boundary layer on the upstream portion of the cylinder similar to the effect of free stream turbulence. Here, the augmentation of α was more pronounced for the case of lower frequency.

In a more recent heat transfer study (Gopinath & Harder, 2000), a preheated 5-mm cylinder was exposed to acoustically imposed low-amplitude zero-mean oscillatory flows to investigate the mechanisms of heat transfer from the cylinder at frequencies of 585 to 1213 Hz. Two distinct flow regimes were found to be important. The first one is the attached flow regime which show the expected square root dependence of the Nusselt number, Nu on the appropriate Reynolds number, Re. The second regime is predicted to be an unstable regime in which vortex shedding is prevalent, contributing to higher transfer rates so that the Nu number becomes proportional to $Re^{0.75}$. These findings are in good agreement with those reported in the above mass transfer studies.

The similar relationship between Nu and Re results has been obtained in another recent study (Uhlenwinkel et al., 2000) on much higher frequencies, 10 and 20 kHz. The heat transfer rate was determined by using cylindrical hot-film/wire probes positioned in the acoustic field of strong standing waves. The Nusselt number was found to increase as the 0.65 power of the Reynolds numbers. The experiments revealed a 25-fold increase in the heat transfer rate compared to that of free convection regardless of frequency in the range examined. Because the authors used rather high displacement amplitudes of sound waves and very small probes, the Strouhal number in their experiments should be more than unit suggesting the above- mentioned vortex formation and shedding. This is assumed to be the main reason of why the acoustic effect was so great in this study.

The above results can be summarized as follows. The amplitude of acoustic oscillations plays a crucial role in the enhancement of mass transfer from objects like particles and cylinders. That was the main reason why most of the above-mentioned effects were observed under the resonance acoustic oscillations. The mass transfer coefficient is increased in proportional to the 0.5~1.0 power of the velocity amplitude with a tendency for the power to become close to 0.5 at larger Strouhal numbers (acoustic streaming controlling regime) and to increase up to 1 at smaller Strouhal numbers (vortex shedding controlling regime). The effect of frequency was less pronounced. Moreover, there is a lack of agreement in the literature on the sign of this effect. There are reports showing increase, decrease and no effect of frequency on the mass- heat transfer rates.

It is to be noted that all the above studies dealt with the objects which were fixed in position in the acoustic fields. In actual practice, particles, no matter whether they are purposely added or generated during a process, can be entrained in the flow of the surrounding gas. Moreover, when the airborne particles are exposed to an acoustic field, they can be forced to oscillate on the same frequency as the acoustic field. Both types of particle motion can affect the mass transfer rate remarkably. However, because of the great experimental difficulties, to the best of our knowledge there have not been any experimental studies in this area.

3.2 Improvements in fuel combustion efficiency

These above-mentioned and other findings have motivated extensive research on the application of acoustic oscillations to improve the process performances in combustion, environmental and waste treatment technologies. The results obtained have strongly

suggested that acoustic oscillations offer very attractive possibilities for designing novel processes with improved combustion efficiency and low pollutant emission. These findings would be of considerable interest for experts dealing with such energy intensive industrial processes as metallurgy, material recycling and waste treatment. Below is a brief survey of some recent results presenting the acoustic effects on the combustion efficiency and pollutant emission.

The results of one of the first study in this field (Kumagai & Isoda, 1955) revealed that an imposition of sound vibrations on a steady air flow yields about 15% augmentation of a single fuel droplet burning rate compared to the conventional one. The sound effects was found to be independent of the vibration frequency. More recently, Blaszczyk (Blaszczyk, 1991) investigated combustion of acoustically distributed fuel droplets under various frequencies. The conclusion was that about 14% increase in fuel combustion rate can be achieved at the 120~300 Hz frequency range despite the sound intensity was relatively low, 100~115 dB.

The influence of acoustic field on the evaporation/combustion rates of a kerosene single fuel droplet was investigated experimentally under standing wave conditions (Saito et al., 1994). The authors concluded that the rate increased by 2~3 times when the droplet was fixed at a velocity antinode position of the wave at frequencies < 100 Hz and relatively low sound pressure levels of 100 ~110 dB.

Effects of acoustic oscillations on evaporation rate of methanol droplets (diam.50~150 μm) at room temperatures were investigated in another study (Sujith et al., 2000). The authors found that a 100% increase in the evaporation rate can be obtained only in the presence of a high intense acoustic field at a SPL of 160 dB. There was a weak tendency toward an increase of the effect with frequency ranging from 410 to 1240 Hz. It is to be note that most of the above data support the mechanism in which the obtained enhancement of liquid fuel combustion occurs due to a better mixing between the fuel vapor and oxidant at the droplet interface.

Approximatelly the same effects of acoustics were found on the combustion of solid fuel particles. Yavuzkurt et al. (Yavuzkurt et.al., 1991a) investigated the effect of an acoustic field on the combustion of coal particles in a flame burner by injecting the particles of 20~70 μm into the burning gas stream and by monitoring the light intensity emitted from the flame. Averaged values of light intensity were 2.5~3.5 times higher at SPL of 145~150 dB and frequency of 2000 Hz compared to those without sound application. Additionally, the authors performed a numerical simulation of combustion phenomena of 100-μm coal particles, the results of which revealed 15.7 and 30.2 percent decreases in the char burn-out time at frequency of 2000 Hz and sound intensity levels of 160 and 170 dB, respectively (Yavuzkurt et.al., 1991b). The main reason for the char burning enhancement is that the high-intensity acoustic field induces an oscillating slip velocity over the coal particles which augments the heat and mass transfer rates at the particle surface.

Four loudspeakers were used to apply an acoustic field to 125-μm black liquor solid particles, injected into a reactor tube at a gas temperature of 550^{O}C (Koepke & Zhu, 1998). The intensity of the field was 151 dB, frequency was ranged from 300 to 1000 Hz. The results revealed a 10 percent reduction of char yield compared with that obtained without acoustic field application. Besides, significantly increased yields of product gases CO and CO_2 were also observed with acoustic treatment. On the whole, the results revealed that the acoustic effects were more pronounced for the initial period of particle heat-up. The above two works (Yavuzkurt et.al., 1991a; Koepke & Zhu, 1998) also include brief overviews of earlier publications on the acoustically improved fuel combustion.

3.3 Reduction of combustion-related pollutant emission

In parallel with the combustion enhancement, forced acoustic oscillations provide a way to significantly reduce emission of such pollutions as NO_x,CO and soot particulates. Especially, a large body of literature has been published on suppressing the NO_x formation due to acoustically or mechanically imposed oscillations. Good reviews on this topic can be found in the relevant literature, for example (Hardalupas & Selbach, 2002; Mcquay et al., 1998; Delabroy et al., 1996). NO_x reduction level was found to be strongly dependent on the experimental conditions. The reported values are ranged from 100%(Delabroy et al.,1996) to 15% (Keller et al.,1994) decrease in NO_x emission rate as compared with that for steady flow conditions. The suppression mechanism has been well established. A sound wave, being propagated through a gas, can be thought as turbulent flow fluctuations of certain scale and amplitude which are governed by the wave frequency and intensity, respectively. Thus, imposing acoustic oscillations on flame front enhances the turbulent mixing resulting in reduced peak temperatures at the front that, in turn, is the reason of reduced emission of thermal NO_x. When acoustic field is imposed upon flame containing liquid/solid particles, oscillations of gas around the particles provide an additional mechanism of the peak temperature reduction due to convection. One more reason of low NO_x emission is that high amplitude acoustic oscillations induce a strong recirculation of flue gas inside the combustion chamber. This results in entrainment of the already formed NO_x into the flame zone where NO_x is reduced by hydrocarbon radicals homogeneously or heterogeneously on the surface of carbonaceous solid particles.

The same mechanism causes lowering of emission of CO and other gaseous pollutants although the literature on this subject is much less than that on the NO_x emission control. For example, a large decrease in NO and CO emissions was observed in the presence of acoustic oscillations imposed to an ethanol flame in a Rujke tube pulse combustor (Mcquay et al., 1998). Taking concentration values at steady conditions as a reference, the decreases were 52 ~100% for NO and 53~90% for CO depending on SPL (136 to 146 dB), frequency(80 to 240 Hz) and excess air (10 to 50%). Another example is the work (Keller et al., 1994) the authors of which obtained emissions levels of a premixed methane-air flame below 5 ppm for NO_x and CO.

Few studies examined the effect of forced acoustics on soot emission from different types of flame: a spray ethanol flame of a Rijke tube combustor (Mcquay et al., 1998), acetylene (Saito et al.,1998) and methane diffusion flames (Demare & Baillot, 2004; Hertzberg, 1997). The oscillation frequencies were also different: 200 Hz (Demare & Baillot, 2004), 40~240 Hz (Mcquay et al., 1998), < 100 Hz (Saito et al., 1998) and 40~1000 Hz (Hertzberg, 1997). In spite of such different conditions, all the authors reported full disappearance of soot emission from the flames with acoustic excitation. The results of these studies suggested that acoustic oscillations enhance the mixing of fuel and ambient gas that causes a re-oxidation of soot particles at the flame zone.

4. Pyrometallurgical applications

Another promising area of airborne sonoprocessing is pyrometallurgy. As has been mentioned in the introductory section, several important chemical reactions in pyrometallurgical processes occur at the interface between gas and molten bath under gas-phase mass-transfer control. An important feature of these processes is that many of them use a high speed gas jet to promote the chemical reactions between the gas and molten

metal. Taken together, these features provide the basis for designing a low-cost and high-performance method of sonoprocessing.

The first attempt to use the energy of sound waves for enhancing the rates of pyrometallurgical processes was made in the former Soviet Union in the steelmaking industry. High-intense acoustic oscillations were applied to a basic oxygen converter, that is the most powerful and effective steelmaking process. For a better understanding of the following discussion, the main features of converter process will be explained in more details.

A schematic diagram of a converter process is shown in Figure 3. Iron-based solid scrap and molten pig iron containing 4%C, 0.2~0.8%Si, minor amount of P and S, are charged into a barrel-shaped vessel. Capacity of the vessel can be as large as 400 tons. Fluxes (burnt lime or dolomite) are also fed into the vessel to form slag, which absorbs impurities of P and S from scrap and iron. A supersonic jet of pure oxygen (1) is blown onto the molten bath (2) through a water-cooled oxygen lance (3) to reduce the content of carbon, dissolved in the molten metal, to a level of 0.3~0.6% depending on steel grade. For a high efficiency of the process, the oxygen flow rate must be very high, several normal cubic meters per minute per ton of steel. Impingement of such a high-speed jet upon the molten metal bath is attended by deformation of its surface producing a pulsating crater in the molten metal and causing splashing of the metal at the crater zone as schematically shown in Fig. 3. Typically, the process takes about 20 minutes.

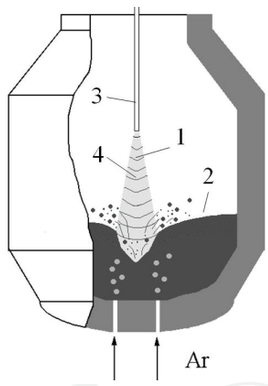

Fig. 3. A schematic representation of converter process.

The oxidation of carbon, which is often termed decarburization, is the main reaction in converter process. The decarburization reaction can proceed in two possible ways. The first one is the direct oxidation by gaseous oxygen according to

$$[C] + 0.5O_2 = CO \tag{23}$$

The second way is the indirect oxidation via formation of iron oxide according to

$$[Fe] + 0.5O_2 = (FeO) \tag{24}$$

$$(FeO) + [C] = [Fe] + CO \tag{25}$$

Here, parentheses and square brackets denote matters dissolved in the slag and metal, respectively. The reactions (23) occurs under the gas-phase mass transfer control. The reaction (24) is controlled by mass transfer of oxygen in both the gas and liquid phases. The

decarburization reaction occurs with a vigorous evolution of CO gas. As a results the slag is foamed and the lance tip becomes submerged into the metal-slag emulsion.
In an attempt to enhance the gas-phase mass transfer rate, an acoustically assisted converter process has been tested. In the process, a pneumatic sonic generator of the Hartmann type was built in the tip of a oxygen lance of a 10-t pilot converter (Blinov, 1991; Blinov & Komarov, 1994). Hence, the sound waves (4) propagated to the molten bath through the gas phase inside the converter as shown in Fig. 3. Design and operating principle of the Hartmann generators was briefly described in our previous review (Komarov, 2005). For the more details, the reader is referred to the earlier publications (Borisov, 1967; Blinov, 1991). The working frequency of sonic generator was 10 kHz. The intensity measured at a distance of 1 m from the generator was 150 dB.

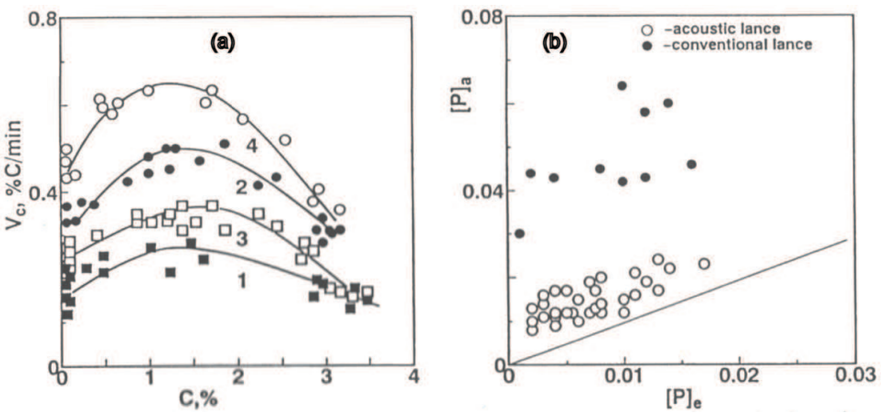

Fig. 4. Dependence of decarburization rate on carbon content (a) and relationship between actual and equilibrium content of phosphorus in the melt after completing the blowing operation.

Figure 4(a) presents the decarburization rate as a function of carbon content for two oxygen flow rates, 4(1,2) and 7(3,4) $Nm^3/min \cdot t$ and two oxygen lances: 1,2 - conventional lance, 3,4 - acoustic lance. The shape of the curves is typical for the decarburization rate in converter process: at the beginning, the rate increased as the carbon content reduced, passed through a maximum and then decreased. As can be seen from this figure, there is a significant effect of the acoustic oscillations on the decarburization rate. This effect seems to be stronger in the intermediate stage of the process while the carbon content is ranged from 0.5 to 2.5%. In the first and final stages of oxygen blowing operation, the effect of acoustic oscillations becomes less pronounced. The average enhancement of decarburization rate due to the acoustic lance application was about 40% under the given test conditions.
It is interesting to note that, in parallel with the enhancement in decarburization rate, there also has been a rise in the efficiency of phosphorus removal from the metal as well when the acoustic oscillations are applied. This reaction can be expressed as follows (Oeters, 1994)

$$[P] + 2.5(FeO) + 1.5(CaO) = 0.5Ca_3(PO_4)_2 + 2.5[Fe] \quad (26)$$

The controlling mechanism of this reaction is more complicated compared to the decarburization reaction, however, it is well known that higher concentrations of FeO in slag is promote the reaction (26). Figure 4(b) is a plot of actual phosphorus concentration,

$[P]_a$ versus equilibrium one, $[P]_e$ for conventional and acoustically assisted process. The values of $[P]_a$ were measured by analyzing metal samples taken at the end of oxygen blow. The equilibrium values were determined according to the theory of regular solution based on the measurements of slag composition at the final stage of the blowing operation (Ban-Ya, 1993). Figure 4(b) shows that equilibrium for the phosphorous distribution between the metal and slag is not attained in the conventional process. This implies that a considerable amount of phosphorus remains in the metal. However, the use of the acoustic lance for blowing operation makes the phosphorous distribution closer to the equilibrium state, as can be seen from Fig. 4(b). Thus, acoustic oscillations were found to be capable of improving the efficiency of both the decarburization and phosphorus removal reactions.

To elucidate possible mechanisms of these improvements, two sets of laboratory scale experiments have been performed. In the first one, an effect of acoustic oscillations on the generation of drops in the above-mentioned crater zone was investigated by using cold models. The second set was aimed at clarifying the gas-phase mass transfer mechanism when the free surface of a liquid is exposed to acoustic oscillations. Below is some details on the experimental procedure and results.

4.1 Generation of drops

It has been known that the intensive drop formation occurs when a gas jet impacts with the gas-liquid interface. To investigate the drop formation a number of lances was designed to perform cold model experiments taking into consideration of the acoustic, aerodynamic and hydrodynamic similarity. In the experiments, the lances were installed vertically at a 0.1-m distance from the free surface of a 0.1-m depth water bath filled in a cylindrical vessel of 0.28 m in inner diameter. Air was blown onto the bath surface to cause a crater formation and drop generation. The drops were detached from the crater surface and carried away from the crater by the gas flow towards the vessel wall where they were trapped by a helical spout. Acoustic oscillations were generated using a specially designed small-scale pneumatic sonic generator of the Hartmann type operating at a frequency of 10 kHz. The generator was positioned above the water bath surface at such a distance that to obtain approximately the same sound pressure level at the crater as that during the pilot converter tests. Magnitude and frequency of turbulent oscillations was measured by using hot wire anemometry. The sensor was fixed close to the gas-liquid interface at the places free of the drop generation. Besides, a small hydrophone was used to measure frequency of oscillations generated in the water bath near the crater. The hydrophone was fixed in the water bath at a depth of 5 cm from the undisturbed free surface. More details on the experimental setup, procedure and results can be found in the following references (Blinov, 1991; Blinov & Komarov, 1994). Below is a brief description of the experimental results.

Magnitude of turbulent oscillations, ε_t was in direct proportion to the gas jet speed. The generation of drops began as ε_t reached a threshold value, irrespective of whether the acoustic oscillations are applied or not. There was a tendency for the threshold value to slightly reduce with the sound wave application. In either case, once begun, the drop generation continues with the rate rising proportionally to ε_t. On the whole, the application of acoustic oscillations caused the drop generation rate to increase by 20~50% depending on the lance design.

One possible explanation for the drop generation mechanism and the acoustic effect on it is as follows. A gas flow reflected from the interface enhances the horizontal component of flow velocity in the liquid near the impact zone. As the gas flow velocity is very high, a high

level of turbulent oscillations are generated in the flow. The turbulent oscillations disturb the gas-liquid interface that results in the formation of capillary waves. The separation of a drop happens at the instant at which the wave amplitude exceeds a threshold value, A_c. This is schematically shown in Figure 5, where A denotes the amplitude of the first largest crest of the wave. This amplitude is the following function of kinematic viscosity, ν and wave length, λ (Tal-Figiel, 1990)

$$A = \frac{4\nu}{f\lambda} \tag{27}$$

Note that here f is the frequency of oscillations generated in water.
The drop formation becomes possible at a threshold amplitude of capillary wave, A_c

$$A_C \geq (4 \sim 7)A \tag{28}$$

The length of a capillary wave can be found from the following equation (Tal-Figiel, 1990)

$$\lambda = \left(\frac{2\pi\sigma}{f^2\rho}\right)^{\frac{1}{3}} \tag{29}$$

where σ is the surface tension of liquid. Substituting this expression into formula (27) Eq.(30) can be obtained.

$$A = 2.169\nu\left(\frac{\rho}{f\sigma}\right)^{\frac{1}{3}} \tag{30}$$

The frequency, *f* was measured by means of the above-mentioned hydrophone.
In the absence of acoustic oscillations, *f* varied over a wide spectrum from 12.5 to 230 Hz, with the fundamental frequency ranging from 135 to 200 Hz. It was found that the fundamental frequency increases twice and more under the application of acoustic oscillations. This phenomenon is assumed to be the main reason for the observed enhancement in drop generation rate due to acoustic oscillations.

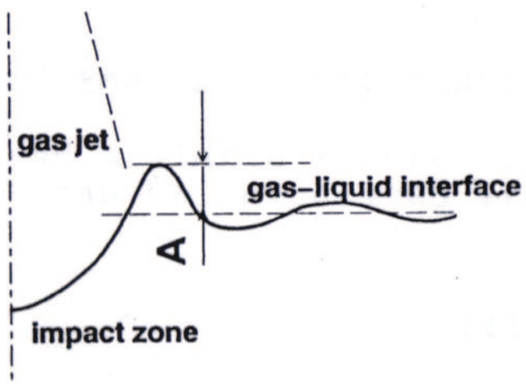

Fig. 5. A shematical representation of gas jet impact.

4.2 Mechanism of acoustically enhanced mass transfer

This section presents results of a cold model study concerning the possible effects of acoustic oscillations on the mass transfer characteristics with special emphasis on the influences of the oscillation frequency. In the experiments, the rates of the following gas-liquid absorption reactions were measured under different experimental conditions

$$2NaOH(aq) + CO_2 = Na_2CO_3(aq) + H_2O \quad (31)$$

$$2Na_2SO_3(aq) + O_2 = 2Na_2SO_4(aq) \quad (32)$$

$$O_2 = O_2(aq) \quad (33)$$

In these equations, aq denotes aqueous solution. A distinguishing characteristic of these reaction is that they proceed under different controlling regimes. The controlling mechanisms of these reactions were examined experimentally. The rate of the first reaction was found to be controlled by the interface mass transfer in both the liquid and gas phases. The second reaction proceeded under mixed control, the chemical reaction and interface gas-phase mass transfer. The rate of the third reaction, physical absorption of O_2 by water, was under the interface liquid-phase mass transfer control.

Figure 6 gives some details on the experimental setup used. This figure was reproduced from our previous paper (Komarov et al., 2007). The above-mentioned aqueous solutions or distilled water were filled into a cylindrical acrylic vessel 0.28 m in diameter and 0.47 m in height covered with an acrylic lid. The depth of the liquid bath was 0.2 m through all experiments. Gas, CO_2-N_2 mixture (reaction 31), air-N_2 mixture (reaction 32) or pure oxygen (reaction 33), was blown onto the liquid bath surface through a vertical tube (I.D.3 mm) fixed at the lid so that the distances between the axis lines of vessel and tube, and between the tube end and bath free surface was 0.02 and 0.13 m, respectively. The liquid bath was agitated by a 6 blade rotary impeller. The impeller was installed vertically at the vessel axis line. The flow rates of blown gas and the rotation speed of impeller were relatively low throughout these experiments. Hence, no drop generation ocurred and the area of the free surface of liquids was assumed to remain unchangeable regardless of the experimental conditions.

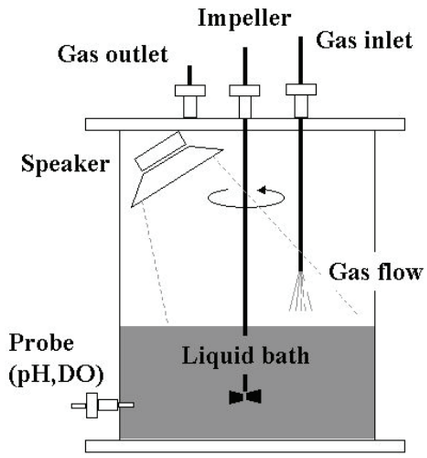

Fig. 6. Experimental setup for investigation of the acoustic effects on the mass transfer characteristics.

Sound waves were generated by using a powerful loudspeaker with the following characteristics: frequency range 70 ~ 18000 Hz, maximum input electrical power 50 W. The loudspeaker was fixed at the vessel lid so that the its vibrating diaphragm was inclined to the liquid free surface at an angle of about 27° as shown in Fig.6. Two broken lines show approximately the sound beam boundaries. The probe shown in the figure was used in order to measure the rates of reactions (31), pH probe, and (33), DO probe. Details on the measurement procedure can be found in our earlier publication (Komarov et al., 2007).

Exposing the gas-liquid interfaces to sound waves resulted in enhancement of the rates of all the above reactions, however the effect was different depending on the sound frequency, sound intensity, conditions of blowing gas and impeller rotation speed. For the reaction of CO_2 absorption, there was a tendency for the decrease in effect of acoustic oscillations as the velocity of blown gas increases and the rotation speed of impeller decreases. At the same gas velocity and rotation speed, the effect of sound for this reaction at a higher frequency was greater than that at a lower one. The largest enhancement in the mass transfer coefficient was 1.8 times at frequency of 15 kHz and gas velocity of 5 m/s. However, the frequency influence was rather complicated. There were frequencies at which the mass transfer coefficient peaked. Additional measurements of sound pressure level in the working space showed that the peaks originated from resonance phenomena occurring inside the vessel at certain frequencies.

The rate of Na_2SO_3 absorption was also enhanced with frequency. The measurements were performed at those frequencies where no resonance phenomena was observed. A 70% augmentation in the absorption rate was obtained within the frequency range of 0~7 kHz at a relatively high velocity of blowing gas, U_g =20 m/s. Therefore, the effect of sound application on this reaction appears to be stronger than that on the CO_2 absorption reaction.

The effect of acoustic oscillations on reaction (33) was significantly smaller as compared to those of reactions (31) and (32). The mass transfer coefficient rose appriximately by 20% as the oscillation frequency increased from 0 to 3 kHz. Notice that such a small effect was obtained at the velocity of blowing gas as low as 2.4 m/s.

Therefore, these three reactions can be arranged in order of increasing effect of sound on the reaction rates in the following way: physical absorption of oxygen by water, CO_2 absorption by NaOH aqueous solution and oxygen absorption by Na_2SO_3 aqueous solution. Thus, the above experimental results suggests definitely that the main reason of the increase in the absorption rates is an acoustically enhanced gas-phase mass transfer.

An analogy between turbulent and acoustic oscillations is thought to provide the best explanation for the mechanisms causing the observed mass transfer enhancement. Lighthill (Lighthill, 2001) was one of the firsts who noticed this analogy. In turbulent flows, fluid particles perform oscillations the amplitude and frequency of which are governed mainly by the flow velocity and the surrounding geometry. Propagation of a sound wave in a fluid medium causes fluctuations of the fluid particles too, with the only difference that they are oscillated at frequencies and amplitudes which are governed by the sound frequency and intensity (or pressure), respectively. This was confirmed by the following measurement results. Figure 7 shows the results of Fourier analysis of turbulent fluctuations generated near the air-water free surface exposed to a sound wave at a frequency of 880 Hz. This figure was reproduced from our previous paper (Komarov et al., 2007). The results make it clear that the fluctuation at the frequency of sound has much higher amplitude than fluctuations at the other frequencies. The measurements were performed at a distance of 2 mm above the surface using a highly sensitive hot-wire anemometry.

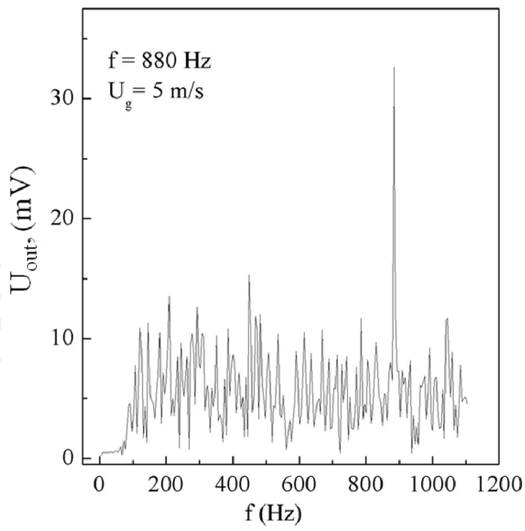

Fig. 7. Fourier analysis results of fluctuations imposed by a sound wave

Based on the above analogy, an attempt was made to explain the effects of sound frequency and intensity using relationships obtained for turbulent fluctuations. Omitting the intermediate transformations, the final expression for mass transfer coefficient, k can be written as follows

$$k \propto Sc^{-\frac{2}{3}} V_a^{\frac{1}{2}} \omega^{\frac{1}{4}} \tag{34}$$

where Sc is the Shmidt number (=ν/D), ν and D is the kinematic viscosity and diffusion coefficient, respectively, V_a is the average amplitude of velocity oscillations in acoustic boundary layer and ω is the angular frequency (=2πf). The thickness of acoustic boundary layer,δ is determined from Eq.(17). The underlying assumptions in deriving expression (34) were that, firstly, a viscous dissipation of acoustic oscillations occurs within the acoustic layer; secondly, the dissipation mechanism in gas phases at the gas-liquid interface is the same as that at the gas-solid interface. Readers interested in more detals are referred to the above-cited paper (Komarov et al., 2007)

Thus, expression (34) shows that the gas-phase mass transfer coefficient should increase with the one-forth power of the sound frequency. When this prediction is compared with the above experimental results, it becomes clear that the experiments show a little weaker frequency dependence. For example, according to the experimental results, the absorption rates of CO_2 and O_2 increased by 1.36 and 1.44 times within frequency ranges of 3 ~15 kHz and 1~7 kHz, respectively. However, for these frequency ranges, relationship (34) predicts enhancement in k by 1.5 and 1.63 times, respectively. The reason of why the experiments show less enhancement effect as compared with the predictions is that the above two reactions are controlled by the gas-phase mass transfer rate only in part as it has been explained in the previous sections.

Also, relationship (34) reveals that mass-transfer coefficient is proportional to the square root of oscillatory velocity amplitude, Va, that is considered to be a characteristic of sound field pressure. However, experimental verification of this prediction presents a considerable difficulty under the present experimental conditions. The reason is that, since sound waves

propagate inside the vessel, they experience multiple reflections from both the free surface of liquid and vessel wall that causes resonance-like phenomena. This results in appearance of the above-mentioned maximums of mass transfer coefficient at certain frequencies, and makes it difficult to measure the sound pressure at the free surface of water bath.

As it has been briefly mentioned above, the effect of acoustic oscillations on mass transfer rate reduces with increasing the velocity of gas blown onto the free surface. This tendency is readily apparent from the finding that both the gas flows and sound waves produce turbulent oscillations at the gas-liquid interface. In high temperature processes, which use high velocity gas jets, the turbulence level in the gas phase should be very high. Under such conditions, the acoustic effects should be weak. Therefore, it would be interesting to estimate the threshold amplitudes of sound waves at which they are still effective in enhancing the gas-phase mass transfer for a given magnitude of the gas turbulent oscillations.

These estimates were made by considering two types of turbulent diffusion coefficients at the gas-liquid interface: that which originates from natural turbulent fluctuations of high speed gas flow, D_t and that which results from imposed acoustic oscillations, D_a. The expressions for these coefficients have been derived in the following form (Komarov et al., 2007)

$$D_t = \frac{0.4\rho v_t^3}{\sigma} z^2 \tag{35}$$

$$D_a = 0.8 V_0 k z^2 \tag{36}$$

where ρ is the density of gas, σ is the surface tension of liquid, v_t is the characteristic turbulent velocity, V_0 is the amplitude of oscillation velocity, k is the wave number of sound wave and z is the distance from the liquid surface.

By equating D_t with D_a, one can obtain a threshold velocity amplitude of sound wave, V_0^* at which the effects of natural turbulence and acoustically imposed oscillations on the gas phase mass-transfer rate are equal.

$$V_0^* = \frac{\rho v_t^3}{2k\sigma} \tag{37}$$

This expression suggests the following. First, in high intensity turbulent flows, the sound waves should have very high oscillation amplitudes in order to be effective. Second, the threshold velocity amplitude decreases with increasing the sound frequency if the other parameters are fixed. Recall that the wave number is proportional to sound frequency as described in the section 2.1.

Using Eq.(37), one can estimate V_0^* for conditions of the present cold model experiments and pilot converter tests. The estimate results are shown in Fig. 8 as plots of V_0^* versus v_t for the cold model at frequencies of 1 (line 1) and 10 kHz (line 2), and for the pilot converter at a frequency of 10 kHz (line 3), respectively. Two right vertical axes indicate the sound intensity level (SIL) in decibel units determined according to Eq.(5). This figure was reproduced from our previous paper (Komarov et al., 2007).

The following values of the physical properties were used in the estimates: ρ = 1.2 kg/m^3 and σ = 0.07 N/m for air-water system at 20°C, and ρ = 0.18 kg/m3 and σ = 1.4 N/m for the

converter process including a CO gas atmosphere and molten steel at 1600°C. The sonic speeds were taken to be equal to 340 and 860 m/s for room and high temperatures, respectively. The shaded areas indicate the approximate ranges of the variation in v_t and V_0^*. The characteristic turbulent velocity was determined assuming a 5 % level of turbulence relative to the gas velocity at the nozzle exit. For the cold model conditions, the values of SIL were estimated to be 110~130 dB.

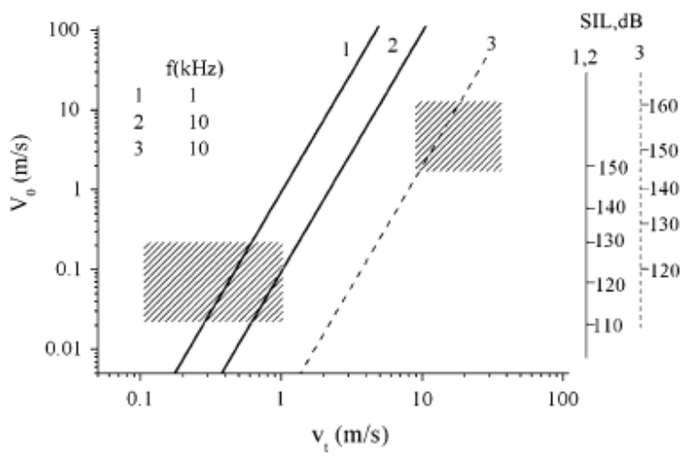

Fig. 8. A plot of V_0 versus v_t: 1 and 2 – cold model, 3 – pilot converter

Estimates of V_0^* for the pilot converter process, assuming that v_t is varied in the range of 10 to 35 m/s, suggest that the acoustic oscillations can be capable of enhancing the mass-transfer rate at sound pressure levels of 145~160 dB and frequency of 10 kHz. These estimates appear to be consistent with the above experimental observations.

Thus, the results presented in this section allow the following conclusions to be drawn. Application of high-intense acoustic oscillations causes the rate of decarburization reaction to enhance. A few mechanisms appear to exist that can result in this enhancement. The first one is the acoustically enhanced generation of drops at the crater zone where the high speed oxygen jet impact with the molten metal bath. The metal drops are oxidized by gaseous oxygen to FeO when flying through the crater zone. The acoustically imposed oscillations enhance the oxidation rate of drops through the above considered intensification of turbulent fluctuations and acoustic streaming at the drop surface. When such oxidized drops are delivered into the slag, its oxygen potential is assumed to become higher as compared with conventional blowing operation. As a result, the rates of decarburization and phosphor removal are enhanced.

4. Concluding remarks

Recently, considerable research efforts have been devoted to the investigation of acoustic oscillations for improving the performance of processes involving high and elevated temperatures. The research results have strongly suggested that the acoustic oscillations have the potential to enhance the efficiency of those processes, the rate of which is controlled by gas-phase mass transfer. Examples include, but not limited to, combustion of liquid and solid fuels, treatment of high temperature exhaust gas, steelmaking converter and Peirce–Smith converter for the refining of cooper. At higher temperatures, attractiveness of

sonic and ultrasonic waves is associated with its ability to propagate through gas, and thus to transfer the acoustic energy from a gas or water cooled ultrasonic generator to a higher temperature area for material processing. Furthermore, if the wave intensity is high enough, its propagation initiates such non-linear phenomena as acoustic streaming, forced turbulence and capillary waves which are the prime causes of acoustic effects, especially at the gas-liquid or gas-solid interfaces.

A survey reveals that amplitude of acoustic oscillations plays a crucial role in the enhancement of gas-phase mass transfer from objects like particles and drops, while the effect of frequency is less pronounced. According the reported results, the mass transfer coefficient is increased in proportional to the 0.5~1.0 power of the velocity amplitude. Two controlling regimes were found to be important: 1- acoustic streaming controlling and 2 - vortex shedding controlling regime.

Experimental results have showed that the high-intense acoustic oscillations are capable of enhancing the rate of gas-phase mass transfer controlling reactions in steelmaking converter process. The following two mechanisms were found to play an important role in this enhancement: 1- acoustically enhanced generation of molten metal drops, 2 – acoustically intensified turbulent fluctuations and acoustic streaming at the drop surface.

Industrial competitiveness of the ultrasonic-based technologies is reinforced by relatively low cost of the power-generating equipment. In some special cases, the acoustic energy can be produced without any additional energy consumption by means of a comparatively simple device. An example is the pneumatic sonic generator applied to a process which uses gas blowing or injection.

5. References

Abramov, O. V. (1998). *High-Intensity Ultrasonics : Theory and Industrial Applications*, Gordon and Breach Science Publishers, ISBN : 9789056990411, Amsterdam.

Abramov, O. V; Khorbenko, S. G. & Shvelga, S. (1984). *Ultrasonic Processing of Materials*, Mashinostroenie, Moscow, [in Russian]

Bird, R. B.; Steart, W. E. & Lightfoot E.N. (2001). *Transport Phenomena*, John Wiley & Sons, Inc., ISBN 0-471-41077-2 , New York.

Blaszczyk, J. (1991). Acoustically disturbed fuel droplet combustion. *Fuel*, Vol.70,No.9, 1023-1025 , ISSN 0016-2361.

Blinov, K. A. (1991). *Application of Acoustic Oscillations for Steelmaking Processes*, Metallurgia, Chelyabinsk, Russia, [in Russian].

Blinov, K. A. & Komarov, S. V.(1994). Liquid dispersion and fine particle coagulation in depevopment of metallurgical processes. *Proceeding of the Second International Symposium on Metallurgical Processes for the Year 2000 and Beyond and the 1994 TMS Extraction and Process Metallurgy Meeting*.pp.413-427, ISBN 10 0873392418, Sxan Diego, California, September 20-23, TMS, Warrendale, Pa.

Borisov, Yu. Ya. (1967). Hartmann type gas-jet oscillators, In : Source of Power Ultrasound, Rozenberg L.D. (Ed.), 7-110,Nauka,Moscow [in Russian].

Carlson, J & Martinsson, P. E.(2002). A Simple Scattering Model For Measuring Particle Mass Fractions In Multiphase Flows. *Ultrasonics*, Vo.39,585-590, ISSN 0041-624X

David, J & Cheeke, N. (2003). *Fundamentals and Applications of Ultrasonic Waves*, CRC Press,ISBN 9780849301308, Boca raton.

Delabroy, O.; Lacas, F.; Poinsot, T.; Candel, S.; Hoffmann, T.; Hermann, J.; Gleis, S. & Vortmeyer, D .(1996). A study of NOx reduction by acoustic excitation in a liquid fueled burner. *Combustion Science and Technology,* Vol.119, 397-408, ISSN 0010-2202.

Demare, D. & Baillot, F. (2004). Acoustic enhancement of combustion in lifted nonpremixed jet flames. *Combustion and Flame,* Vol.139,No.4, 312-328, ISSN 0010-2180.

Fand,R.M. & Cheng,P.(1962). The Influence of Sound on Heat Transfer from a Cylinder in Crossflow. *Int.J.Heat Mass Transfer*, Vo.6, 571-596, ISSN 0017-9310.

Gopinath,A. & Mills, A.F.(1994). Convective Heat Transfer Due to Acoustic Streaming Across the Ends of Kundt Tube. *Journal of Heat Tranfer*,Vo.116, 47-53, ISSN 1528-8943

Hamilton, M. F & Blackstock, D. T. (1998). *Nonlinear Acoustics, Theory and Applications*, Academic Press, ISBN : 0123218608 , California

Hardalupas, Y. & Selbach, A. (2002). Imposed oscillations and non-premixed flames, Prog Energ Combust, Vol.28, 75-104, ISSN 0360-1285.

Hertzberg, J. (1997). Conditions for a Split Diffusion Flame. *Combustion and Flame*, Vol.109, 314-322, ISSN 0010-2180.

Hueter, T. F. & Bolt, R. H. (1966). *Sonics*, John & Sons, Inc., ISBN, New York

Kawahara, N.; Yarin, A. L.; Brenn, G.; Kastner, O. & Durst, F. (2000). Effect of acoustic streaming on the mass transfer from a sublimating sphere. *Physics of Fluids*, Vo.12.,No.4 ,912-923, ISSN 1070-6631.

Keller, J. O.; Bramlette, T. T.; Barr P.K. & Alvarez J. R.(1994). NO_x and CO emissions from a pulse combustor operating in a lean premixed mode. *Combustion and Flame,* Vol.99, 460-466, ISSN 0010-2180.

Koepke, S. A & Zhu, J. Y. (1998). Pyrolysis of Black Liquor in a High-intensity Acoustic Field. *Combustion Science and Technology,* Vol.140, 315-331, ISSN 0010-2202.

Komarov,S.V.; Kuwabara, M.& and Abramov, O.V. (2005). High Power Ultrasonics in Pyrometallurgy: Current Status and Recent Developments. *ISIJ International*, Vol. 45, 1765-1782, ISSN 0915-1559.

Komarov, S. V.; Noriki, N.; Osada, K.; Kuwabara, M. & Sano, M. (2007). Cold Model Study on Mass-Transfer Enhancement at Gas-Liquid Interfaces Exposed to Sound Waves. Metallurgical and Materials Transactions, Vol.38B, 809-818, ISSN 1073-5615

Kumagai, S. & Isoda, H. (1955). Combustion of Fuel Droplets in a Vibrating Air Field. *Proceeding the Fifth International Symposium on Combustion*, pp.129-132, Pittsburgh, May 1955, Reinhold Publishing, New York.

Landau, L. D & Lifshits, E. M. (1986). *Fluid Mechanics,* Nauka, Moscow,Russia [in Russian].

Larsen, P. S. & Jensen, J. W.(1977). Evaporation Rates of Drops in Forced Convection with Superposed Transverse Sound Field. *Int.J.Heat Mass Transfer*, Vo.21, 511-517, ISSN 0017-9310.

Leighton, T. G. (2004). From seas to surgeries, from babbling brooks to baby scans: The acoustics of gas bubbles in liquids. *International Journal of Modern Physics B.,* Vol.18, 3267-3314, ISSN 0217-9792.

Lighthill, J. (1978),Acoustic Streaming. *Journal of Sound and Vibration*, Vo.61, No.3, 391-418, ISSN 0022-460X.Lighthill,J. (2001), *Waves in Fluids*, Cambridge University Press, ISBN 0-521-01045-4, Cambridge.

Loh, B. G. & Lee D. R. (2004). Heat Trabsfer Characteristics of Acoustic Streaming by Longitudinal Ultrasonic Vibration. *J Thermophys Heat Tran*, Vo.18, No.1, 94-99, ISSN 0887-8722

Makarov, S. & Ochmann, M. (1996). Non-linear and thermoviscous phenomena in acoustics. Part I. *Acustica,* Vol.82, 579-606, ISSN 00017884 .

Makarov, S. & Ochmann,M.(1997). Non-linear and thermoviscous phenomena in acoustics. Part II. *Acustica,* Vol.83, 197-222, ISSN 00017884.

Margulis, M.A. (1995). *Sonochemistry and Cavitation*, Taylor & Francis, ISBN: 978-2881248498, Amsterdam.

Mason, W. P. & Thurston, R. N. (1965). *Physical Acoustics*, Vol.4, Part B, Academic Press Inc., New York.

Mcquay, M. Q.; Dubey, R. K. & Nazeer, W. A. (1998). An experimental study on the impact of acoustics and spray quality on the emissions of CO and NO from an ethanol spray flame. *Fuel,* Vol.77, 425-435, ISSN 0016-2361.

Mednikov, E. P. (1965). *Acoustic coagulation and precipitation of aerosols* (authorized translation from the Russian by Chas V. Larrick), USSR Academy of Sciences Press, Moscow.

Oeters, F. (1994). *Metallurgy of Steelmaking.* pp.47-54, Stahleisen, Dusseldorf

Rayleigh, J. W. S. (1945). *Theory of Sound*, Vol.1,2. Dover Publications, N.Y.

Saito, M.; Sato, M. & Suzuki, I. (1994). Evaporation and combustion of a single fuel droplet in acoustic fields. *Fuel*, Vol.73, No.3, 349-353 , ISSN 0016-2361.

Saito, M.; Sato, M. & Nishimura, A. (1998). Soot suppression by acoustic oscillated combustion. *Fuel,* Vol.77, No.9-10, 973-978, ISSN 0016-2361.

Sujith, R. I.; Waldherr, G. A.; Jagoda, J. I. & Zinn, B. T. (2000). Experimental Investigation of the Evaporation of Droplets in Axial Acoustic Fields, *Journal of Propulsion and Power*, Vo.16, 278-285, ISSN 0748-4658.

Sung, H. J.; Hwang, K. S. & Hyun, J.M. (1994). Experimental Stydy on Mass Transfer from a Circular Cylinder in Pulsating Flow. *Int.J.Heat Mass Transfer*, Vo.37, No.15, 2203-2210, ISSN 0017-9310.

Tal-Figiel, B. (1990). Conditions for instability of the liquid-liquid interface in a ultrasoinc field. *International Chemical Engineering*, Vo.30, No.3, 526-534, ISSN 1385-8947.

Temkin, S.(1998).Sound propagation in dilute suspensions of rigid particles. *J. Acoust. Soc.Am*, Vol.103, No.2,838-849, ISSN 0001-4966

Uhlenwinkel, V.; Meng, R. & Bauckhage, K. (2000). Investigation on heat transfer from circular cylinders in high power 10 kHz and 20 kHz acoustic resonant fields. *Int.J.Therm.Sci.*, Vo.39, 771-779, ISSN 1290-0729.

Vainstein, P.; Fichman, M. & Gutfinger, C.(1995). Acoustic Enhancement of heat transfer between two parallel plates. *Int.J.Heat Mass Transfer*, Vo.38, No.10, 1893-1899, ISSN 0017-9310

Yarin, A. L.; Brenn, G.; Kastner, O.; Rensink, D. & Tropea, C. (1999). Evaporation of acoustically levitated droplets. *J. Fluid Mech.*, Vol.399, 151-204, ISSN 0022-1120.

Yavuzkurt, S.; Ha, M. Y.; Koopman, K. & Scaroni, A. W. (1991,a). A Model of the Enhancement of Coal Combustion Using High-Intensity Acoustic Fields. *Journal of Energy Resources Technology*, Vol.113, No.4, 277-285, ISSN 0195-0738.

Yavuzkurt, S.; Ha, M. Y.; Reethof, G.; Koopmann, G. & Scaroni, A. W.(1991,b). Effect of an acoustic field on the combustion of coal particles in a flat flame burner. *Journal of Energy Resources Technology,* Vol.113, Vol.4, 286-293, ISSN 0195-0738.

Zarembo, L. K. (1971). Acoustic streaming. In : *High-Intensity Ultrasonic Fields*, Rozenberg L.D. (Ed.), 137-199, Plenum, New York.

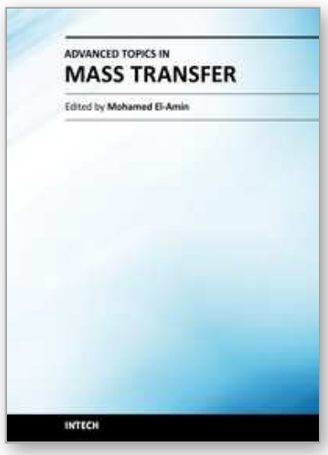

Advanced Topics in Mass Transfer

Edited by Prof. Mohamed El-Amin

ISBN 978-953-307-333-0
Hard cover, 626 pages
Publisher InTech
Published online 21, February, 2011
Published in print edition February, 2011

This book introduces a number of selected advanced topics in mass transfer phenomenon and covers its theoretical, numerical, modeling and experimental aspects. The 26 chapters of this book are divided into five parts. The first is devoted to the study of some problems of mass transfer in microchannels, turbulence, waves and plasma, while chapters regarding mass transfer with hydro-, magnetohydro- and electro- dynamics are collected in the second part. The third part deals with mass transfer in food, such as rice, cheese, fruits and vegetables, and the fourth focuses on mass transfer in some large-scale applications such as geomorphologic studies. The last part introduces several issues of combined heat and mass transfer phenomena. The book can be considered as a rich reference for researchers and engineers working in the field of mass transfer and its related topics.

INTECH
open science | open minds

InTech Europe
University Campus STeP Ri
Slavka Krautzeka 83/A
51000 Rijeka, Croatia
Phone: +385 (51) 770 447
Fax: +385 (51) 686 166
www.intechopen.com

InTech China
Unit 405, Office Block, Hotel Equatorial Shanghai
No.65, Yan An Road (West), Shanghai, 200040, China
中国上海市延安西路65号上海国际贵都大饭店办公楼405单元
Phone: +86-21-62489820
Fax: +86-21-62489821

IntechOpen